Geophysical Research Letters

RESEARCH LETTER
10.1029/2022GL099520

Key Points:

- Three million years of continuous land surface temperatures reconstructed based on soil bacterial lipids
- The land temperature record indicates an unexpected warming trend over the Pleistocene
- Increasing land-sea thermal contrast facilitated the long-term intensification of Pleistocene East Asian summer monsoon

Supporting Information:

Supporting Information may be found in the online version of this article.

Correspondence to:

W. Liu and H. Yang,
liuwg@loess.llqg.ac.cn;
hyang@bryant.edu

Citation:

Lu, H., Liu, W., Yang, H., Leng, Q., Liu, Z., Cao, Y., et al. (2022). Decoupled land and ocean temperature trends in the early-middle Pleistocene. *Geophysical Research Letters*, *49*, e2022GL099520. https://doi.org/10.1029/2022GL099520

Received 13 MAY 2022
Accepted 16 AUG 2022

Author Contributions:

Conceptualization: Hongxuan Lu, Weiguo Liu
Data curation: Hongxuan Lu, Zheng Wang, Zeke Zhang, Weijian Zhou, Zhisheng An
Formal analysis: Hongxuan Lu, Qin Leng, Zhonghui Liu, Weijuan Sheng, Huanye Wang, Zheng Wang, Youbin Sun, Zhisheng An
Funding acquisition: Hongxuan Lu, Weiguo Liu
Investigation: Hongxuan Lu, Yunning Cao, Jing Hu, Weijuan Sheng
Methodology: Hongxuan Lu, Weijuan Sheng, Huanye Wang
Project Administration: Hongxuan Lu
Resources: Hongxuan Lu
Software: Hongxuan Lu
Supervision: Weiguo Liu, Hong Yang
Validation: Hongxuan Lu
Visualization: Hongxuan Lu

Decoupled Land and Ocean Temperature Trends in the Early-Middle Pleistocene

Hongxuan Lu[1,2], Weiguo Liu[1,2], Hong Yang[3], Qin Leng[3], Zhonghui Liu[4], Yunning Cao[1,2], Jing Hu[1,2], Weijuan Sheng[1], Huanye Wang[1,2], Zheng Wang[1,2], Zeke Zhang[1,2], Youbin Sun[1,2], Weijian Zhou[1,2], and Zhisheng An[1,2]

[1]State Key Laboratory of Loess and Quaternary Geology, Institute of Earth Environment, Chinese Academy of Sciences, Xi'an, China, [2]CAS Center for Excellence in Quaternary Science and Global Change, Xi'an, China, [3]Laboratory for Terrestrial Environments, Department of Science and Technology, Bryant University, Smithfield, RI, USA, [4]Department of Earth Sciences, The University of Hong Kong, Hong Kong, China

Abstract Record of long-term land temperature changes remains ephemeral, discontinuous, and isolated, thus leaving the common view that Pleistocene land temperature evolution should have followed ocean temperatures unconfirmed. Here, we present a continuous land surface temperature reconstruction in the Asian monsoon region over the past 3.0 Myr based on the distribution of soil bacterial lipids from the Chinese Loess Plateau. The land temperature record indicates an unexpected warming trend over the Pleistocene, which is opposite to the cooling trend in Pleistocene ocean temperatures, resulting in increased land-sea thermal contrast. We propose that the previously unrecognized increase of land-sea thermal contrast during much of the Pleistocene is a regional climate phenomenon that provides a likely mechanism in favor of the long-term enhancement of the Pleistocene East Asian summer monsoon.

Plain Language Summary Numerous sea surface temperature (SST) records indicate long-term gradual cooling over the Pleistocene, whereas the East Asian summer monsoon (EASM) appears to have strengthened during this period. Land-sea thermal contrast is thought to have an important influence on the intensity of the EASM, but the lack of land surface temperature (LST) records from monsoonal regions prevents the assessment of its role in driving monsoonal changes. Here, we present a 3-Myr-long LST record from the Chinese Loess Plateau, displaying a unique long-term warming trend over the Pleistocene, different from the trajectories of SST records. We propose that the decoupling of long-term land and sea temperatures, and thus the increase of land-sea thermal contrast, provides a simple interpretation for the otherwise paradox, strengthening of the EASM over the Pleistocene. This study presents much needed original LST data that support novel interpretations on a mechanism for important paleoclimate phenomenon in East Asia with implications to the entire terrestrial ecosystem during the critical period of earth history.

1. Introduction

The current global warming trend has exacerbated our concerns about future changes in land surface temperature (LST), a parameter that has profound impact on terrestrial ecosystems including many aspects of human life (IPCC, 2019). In the quest of better understanding continental climatic changes, documenting and deciphering underlying physical principles of long-term LST evolution in historical periods are critical. However, due to the lack of suitable tools, long-term terrestrial paleotemperature reconstruction is extremely rare, which increases the uncertainty of our projection of future trend for temperature changes. It remains uncertain whether land temperature should have followed the same long-term cooling trend as inferred from marine records over the Pleistocene (Fedorov et al., 2013; Herbert et al., 2010; Lisiecki & Raymo, 2005). In addition, recently reconstructed interglacial rainfall on the Chinese Loess Plateau (CLP) indicated a gradual strengthening of the East Asian summer monsoon (EASM) over the Pleistocene (Balsam et al., 2004; Meng et al., 2018; Tian et al., 2011) against the global cooling climate trend that is mainly inferred from the marine realm, contradicting the long-held convention that high monsoon rainfalls on longer timescales are linked to high global/ocean temperatures. Land temperature records from the region, currently lacking, would also help address this controversy and improve our understanding of the long-term EASM evolution.

Writing – original draft: Hongxuan Lu, Weiguo Liu, Hong Yang, Zhonghui Liu
Writing – review & editing: Hongxuan Lu, Weiguo Liu, Hong Yang, Qin Leng, Zhonghui Liu, Yunning Cao, Jing Hu, Huanye Wang, Zheng Wang, Zeke Zhang, Youbin Sun, Weijian Zhou, Zhisheng An

The loess-paleosol and red-clay sequences on the CLP have been widely accepted as an excellent geologic and climatic archive for documenting the history and variability of the East Asian paleomonsoon climate spanning at least the past 7.2 Myr (T. S. Liu & Ding, 1998). Here, built upon our recent work (Lu et al., 2019), we reconstructed the longest continuous continental paleotemperature history so far based on distributions of soil fossil glycerol dialkyl glycerol tetraether (GDGT; Figure S1 in Supporting Information S1) lipids preserved in well-dated loess-paleosol sequences from the Lingtai section at the center of the CLP (Figure 1). Our result extends the LST reconstruction in Asia to cover the entire Pleistocene and provides critical information toward understanding patterns of continental climatic and environmental changes, allowing us to evaluate the evolutionary history of LST and its intricate relationship with global temperature changes and EASM evolution at the million-year time scale.

2. Materials and Methods

The loess samples were collected from a well-known classic loess profile (Lingtai, 35°04'N, 107°39'E) at the center of the CLP (Figure 1). The age model was constructed by the generally accepted correlation scheme of loess-paleosol sequences with marine benthic oxygen isotopic ($\delta^{18}O$) records (Figures S2–S4 in Supporting Information S1). GDGTs were analyzed on a liquid chromatography/atmospheric pressure chemical ionization-mass spectrometry system. Details were presented in Text S1 in Supporting Information S1.

Based on modern soil data, GDGT-derived proxies offer a promising tool for reconstructing terrestrial temperatures on the CLP (Peterse et al., 2011, 2014; Tang et al., 2017; Wang et al., 2020). The surface soil is more suitable for GDGT producing microorganisms to grow, and thus the GDGT-based temperature reconstructions from loess sections mainly reflect in situ LSTs during the growth season of microorganisms (Lu et al., 2019; Wang et al., 2020). GDGT contents in dust source regions of the CLP contain negligible amount of GDGTs due to their unfavorable growth conditions for bacteria, such as aridity, low temperature, and the lack of organic material (Gao et al., 2012); thus these trace amount of GDGTs adhered to dusts would have little effect on our results. Modern observations have also shown that in northern China across a large climatic gradient affected by these factors, the GDGT indicator has a good relationship with LST (Wang et al., 2020). Besides exogenous input, different calibrations may also have an effect on temperature reconstruction. We compared the reconstructed paleotemperature using different calibrations from global (mean annual air temperature, MAAT) (De Jonge et al., 2014) and regional (China, mean annual soil temperature, MAST) soil data sets (Wang et al., 2020). We found that they have similar trends (Figure 2 and Figure S5 in Supporting Information S1), although the average temperature reconstructed by the former is about 2°C higher than the later, and a higher deviation was observed during colder periods, which is consistent with the modern observation data (Wang et al., 2020). A Bayesian calibration (BayMBT) (Crampton-Flood et al., 2020) and a random Forest Regression for PaleOMAAT using brGDGTs (FROG) calibration (Véquaud et al., 2022) in soils were also proposed to calibrate the relationship of the 5-methyl brGDGTs and the MAAT. However, in the Lingtai loess-paleosol sequence, the IIb and IIc compounds (Figure S1 in Supporting Information S1) required in these two models are usually below the detection limit, so, these two models may be currently inapplicable. Nevertheless, we calculated the temperature with BayMBT by taking the compounds below the detection limit as zero (Figure S5 in Supporting Information S1) and also found that temperature from different calibrations have similar trend. Further discussion about the reliability of brGDGT-based LST reconstructions is provided in Supporting Information S1.

Because bacteria that produce GDGTs mainly live in the surface layer of the soil, the GDGT data more directly reflect the MAST. In addition, compared with global soil data sets, regional temperature calibration has smaller analysis errors. Therefore, we use MAST as our reconstructed LST, and MAT as a reference. An external standard and duplicate injections of a selected set of loess-paleosol samples were analyzed in every 30 samples, and were continuously monitored to ensure minimal analytical drift. The average analytical error, calculated using replicate analyses of external standard and sample duplicates, is 0.8°C (1σ). In addition, error introduced by the temperature calibration is 2.2°C (Wang et al., 2020), thus resulting a combined error up to 3.0°C.

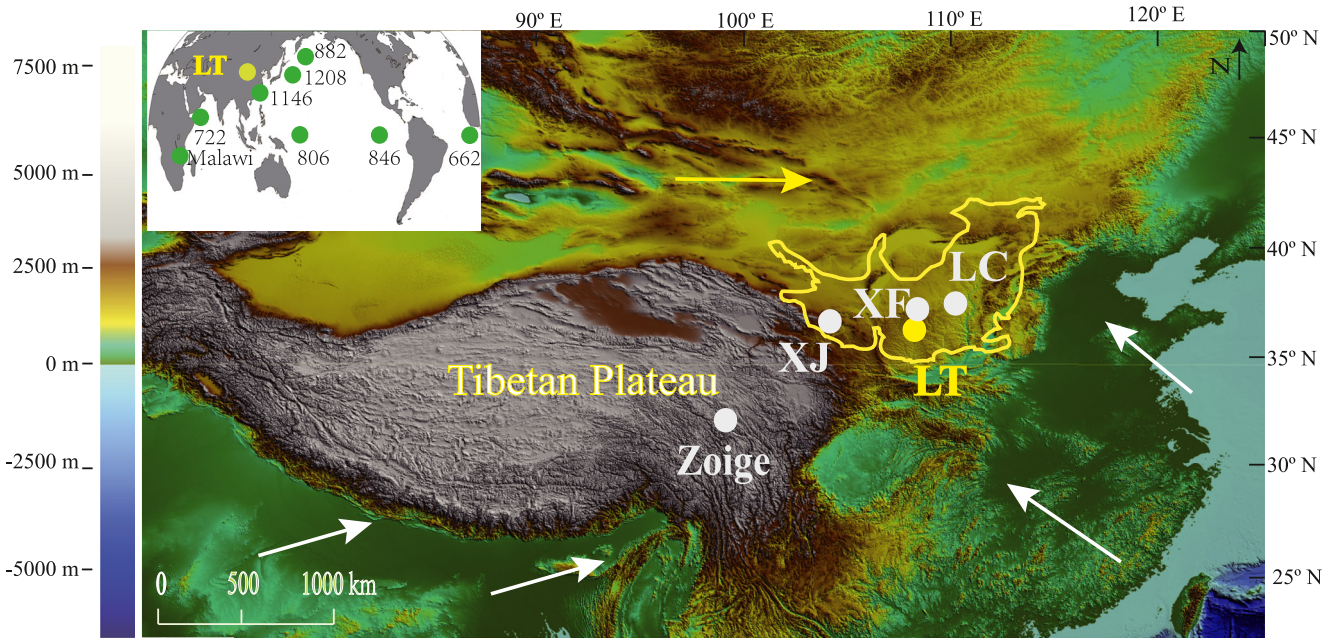

Figure 1. Land relief map of East Asia showing locations of research sites (white circles) near the Lingtai loess-paleosol section (the yellow circle), and other terrestrial and marine (labeled with their ODP number) records used in this study. LC, Luochuan; XF, Xifeng; XJ, Xijin; and LT, Lingtai. Locations of Pleistocene tropical temperature records used in the tropical stack (Herbert et al., 2010) and the two North Pacific records are shown in the inset map. The area enclosed in the yellow line denotes the Chinese Loess Plateau. The yellow (white) arrows indicate the direction of westerlies (summer monsoon) winds. Base map was generated through ArcGIS.

3. Results and Discussion

Our brGDGT-derived new temperature reconstructions extend our paleotemperature records to the past 3 Myr. The record exhibits relatively distinct glacial-interglacial cyclicity that is broadly synchronized with marine $\delta^{18}O$ records in the overall glacial-interglacial pattern (Figure 2 and Figure S4 in Supporting Information S1). Elevated LST occurred in paleosol layers during interglacial periods or weakly developed soil beds in loess layers (such as SS_1 and SS_2 during L_{31}) during glacial periods, while lower temperature values occurred in loess layers during glacial periods, which is highly consistent with previous reports (Lu et al., 2019; Peterse et al., 2011, 2014; Tang et al., 2017; Thomas et al., 2017; Figure 2). However, combined with visual inspection and turning point analysis (Killick & Eckley, 2015), our LST record displays distinct trends at the following three time intervals: (a) 3.0–2.6 Ma, a rapid cooling trend that is similar to sea surface temperature (SST) records (Fedorov et al., 2013), (b) 2.6–0.6 Ma, a gradual warming trend opposite to marine records, and (c) 0.6–0 Ma, a relatively flat trend with large oscillations. The first turning point at ~2.6 Ma coincides with the boundary between the Pliocene Red Clay and Pleistocene loess-paleosol sequence, associated with the global climate during the intensification of the Northern Hemisphere Glaciation (Haug et al., 2005; Sun & An, 2005), changing from relatively warm and humid conditions at the end of the Pliocene to large warm-cold alternations over the Pleistocene. The end of this period around 0.6 Ma is close to the completion of the so-called mid-Pleistocene transition (MPT; 1.2–0.7 Ma), which has been widely recognized as a shift in paleoclimatic periodicity from 41- to 100-Kyr cycles and characterized by significant glacial-interglacial changes in high-latitude ice volume, global ocean temperatures, sea level fluctuations, and monsoonal intensity (Herbert et al., 2010; Lisiecki & Raymo, 2005; Ruddiman et al., 1989; Sun et al., 2006).

Our new LST record highlights several distinct features that are different from the established global marine temperature trends. During the cooling trend interval (3.0–2.6 Ma), the Lingtai GDGT-based paleotemperature shows an accumulative ~3.5°C decrease of temperature on the CLP (Figure 3a), a steeper cooling trend than that has been widely recorded from marine sediments (Fedorov et al., 2013; Herbert et al., 2016; LaRiviere et al., 2012), probably related to the continental intensification of the Northern Hemisphere Glaciation. But one of the most surprising features recorded in our new LST profile is the steady warming trend from ca. 2.6 to 0.6 Ma, as indicated by the 400-Kyr running averages (Figure 3a) or linear fitting (Figure S6 in Supporting

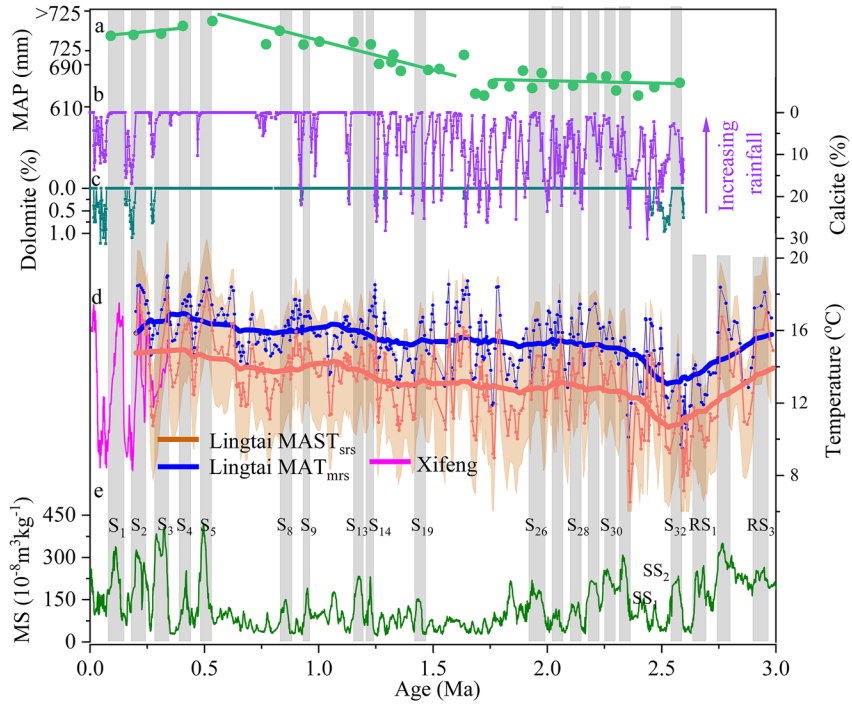

Figure 2. Time series of climatic proxies from the Lingtai loess-paleosol sequence. (a) Mean annual precipitation (MAP) derived from dissolution phases of carbonate, (b) calcite content, and (c) dolomite content (Meng et al., 2018). (d) Glycerol dialkyl glycerol tetraether (GDGT)-derived temperature (Lingtai, orange, three point-moving averaged $MAST_{srs}$, this study; Lingtai, blue, three point-moving averaged MAT_{mrs}, this study; Xifeng, purple, Lu et al., 2019). The shade area in panel (d) represents possible $MAST_{srs}$-derived temperature uncertainty introduced by the GDGT measurements (0.8°C) and the temperature calibration (2.2°C) combined. (e) Magnetic susceptibility (MS). The gray shaded areas indicate paleosol layers, corresponding to interglacial periods. The labels in panel (e) indicate main paleosol layers. The heavy green lines in panel (a) denotes trends in the East Asian summer monsoon (EASM) rainfall. The heavy lines in panel (d) represents 400-Kyr running averages of land surface temperatures. The long-term trend of land warming and EASM enhancement were closely coupled from 2.6 to 0.6 Ma.

Information S1) of the new LST data. A linear regression analysis of our LST data in this period shows that the average temperature has increased by ~1.1°C during these 2 million years, while the average SST at similar latitudes has decreased by ~2.2°C (Herbert et al., 2016). This unique absence of early-middle Pleistocene cooling characteristic in Lingtai LSTs exhibits a sharp contrast with the global average surface temperature change based mainly on SST data (Fedorov et al., 2013; Herbert et al., 2010; Snyder, 2016) (Figure 3), and such a warming LST trend is also in contrast with the change of global atmosphere pCO_2 across the MPT (Chalk et al., 2017). More interestingly, LST changes during glacial and interglacial periods are asymmetric. The warming rate in interglacial paleosol layers (S_{32}–S_6) is ~0.7°C/Myr, while a higher warming rate of ~1.1°C/Myr is recorded in glacial periods in loess layers (L_{30}–L_6) (Figure S6 in Supporting Information S1). The gradual warming trend of LST during 2.6–0.6 Ma documented on the CLP coincides with the increasing of EASM strength recently reported from terrestrial and marine sediments of the same period (Balsam et al., 2004; Meng et al., 2018; Tian et al., 2011). Particularly, the inferred rainfall changes from carbonate and dolomite percentages from the same Lingtai section show close correspondence to LST changes (Figure 2). At about 0.6 Ma, the LST warming trend terminated, and our LST curve is then characterized by the high-amplitude 100-Kyr oscillations, returning to the alignment with other global and regional geochemical proxies, including those for the EASM.

Continuous LSTs spanning over millions of years are extremely rare, making the comparison between our records at CLP with other sites challenging. A 400-Kyr running average of GDGT-based land temperature data from the Malawi valley in Africa (Johnson et al., 2016) shows that the average temperature has increased by ~2.0°C from 1.3 to 0.6 Ma in eastern Africa (Figure 3b) and the warming primarily occurred during glacial periods. Further, a pollen-based temperature record over the last 1.74 Myr from the eastern Tibetan Plateau (Zhao et al., 2021) suggests that, when all modern pollen data from China and Mongolia were used in the training data set, the

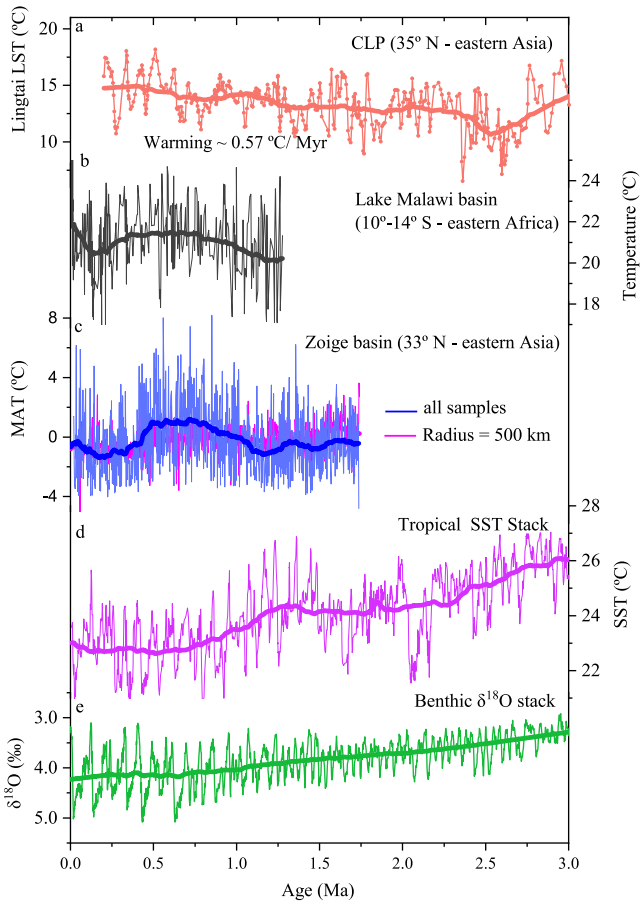

Figure 3. Comparison of continuous temperature records from Chinese Loess Plateau (CLP) and other paleo-records over the past 3.0 Ma, showing increasing divergent land-ocean temperature trends during much of Pleistocene. (a) Land surface temperature (LST) on the CLP, three point-moving averaged. (b) Glycerol dialkyl glycerol tetraether-derived Lake Malawi basin temperature record (Johnson et al., 2016). (c) Weighted-average partial least squares-based temperature reconstructions for Zoige Basin core ZB13-C2 with modern pollen training-set from across China and part of Mongolia (blue) and a smaller modern pollen training-set within a distance of 500 km (red) (Zhao et al., 2021). (d) Tropical sea surface temperature (SST) stack (Herbert et al., 2010). (e) Benthic $\delta^{18}O$ stack (Lisiecki & Raymo, 2005). The heavy lines represent 400-Kyr running averages.

reconstructed mean annual temperature increased substantially between 1.74 and 0.6 Ma, especially between 1.5 and 0.6 Ma (Figure 3c), against the background of global cooling but consistent with our record (Figure 3a). Such high similarity, albeit based upon limited data sets, suggests that the decoupling trends of long-term land and ocean temperatures may not be merely a local coincidence but representing a previously unrecognized long-term regional climate phenomenon during the Pleistocene, particularly in low latitudes to midlatitudes or monsoon-influenced regions.

Deciphering the precise mechanisms for the unexpected Pleistocene land warming may require more continuous continental temperature records. Solar radiation, atmospheric pCO_2, and global ice volume are considered to be the main driving forces of global climate change (Peterse et al., 2011, 2014; Tang et al., 2017; Thomas et al., 2017), but at million-year time scale, these factors cannot explain the long-term land warming trend. While LST records display the fundamental global glacial-interglacial temperature changes, our recent study from the CLP shows that variations of land surface features, such as vegetation and hydrology, may have played an important role in regulating LST for the past 800 Kyr (Lu et al., 2019). In our new record, we still observed that deglacial warming led the magnetic susceptibility changes over glacial-interglacial cycles (Figure S4 in Supporting Information S1), indicating the existence of vegetation effect. Moreover, we note that LSTs were relatively high during some glacial periods, such as loess units L_9, L_{24}, and L_{32} (Figure S4 in Supporting Information S1). Those units, corresponding to relatively cool glacial ocean temperatures (Figure S4 in Supporting Information S1), are usually considered as periods of particularly cold and dry conditions based on physical and chemical proxies analyzed (Sun et al., 2006). Therefore, vegetation effect (Liang et al., 2019; Lu et al., 2019) might have been enhanced during those periods and resulted in elevated LSTs. (Note elevated glacial LSTs were excluded when calculating glacial warming rate).

For the long-term land warming trend over Pleistocene interglacials, based on available land temperature records, we consider that it may represent a regional phenomenon, confined to monsoonal regions, while global climate cooled over the Pleistocene, represented by the SST (Fedorov et al., 2013; Herbert et al., 2010) and pCO_2 records (Chalk et al., 2017). If so, the warming trend in monsoonal regions might have resulted from reorganization of atmospheric circulations, for instance, enhanced tropical Pacific zonal SST gradient and associated processes that corresponded to global cooling. Indeed, the Mg/Ca-SST record from ODP 806B, western equatorial Pacific (Wara et al., 2005), with or without the correction of the seawater Mg/Ca effect (Medina-Elizalde et al., 2008), indicates an overall warming, at least not cooling, trend in interglacial temperatures between 2.6 and 0.6 Ma (Figure 4), consistent with this view. Although a cooling trend appears to be notable between ~1.3 and ~0.9 Ma in this record, this feature is not particularly evident in high-resolution Mg/Ca-SST records over the last ~1.8 Myr in the region (de Garidel-Thoron et al., 2005; Medina-Elizalde & Lea, 2005; Figure 4). The overall warming trend for Pleistocene interglacials in the western Pacific warm pool (overlooked previously) and on the CLP, along with the EASM enhancement, might be all associated with the enhanced tropical zonal SST gradient under the global cooling background. The scenario of increased land-ocean thermal contrast is perhaps consistent with the increased Pacific zonal SST gradient (J. J. Liu et al., 2019; Tierney et al., 2019; Wara et al., 2005; Zhang et al., 2014) as relatively increased heat would have accumulated in the western Pacific which may impact nearby continents. Further, we note that the migration of westerly jet is also associated with EASM development, with enhanced EASM corresponding to a more northern position/weakened westerlies under warmer conditions (Abell et al., 2021; Chiang et al., 2015). However, westerlies appear to have strengthened associated with global cooling over the Pleistocene (Abell et al., 2021; Fang et al., 2020), in contrast with the long-term EASM enhancement. Indeed, this opposite long-term behavior in

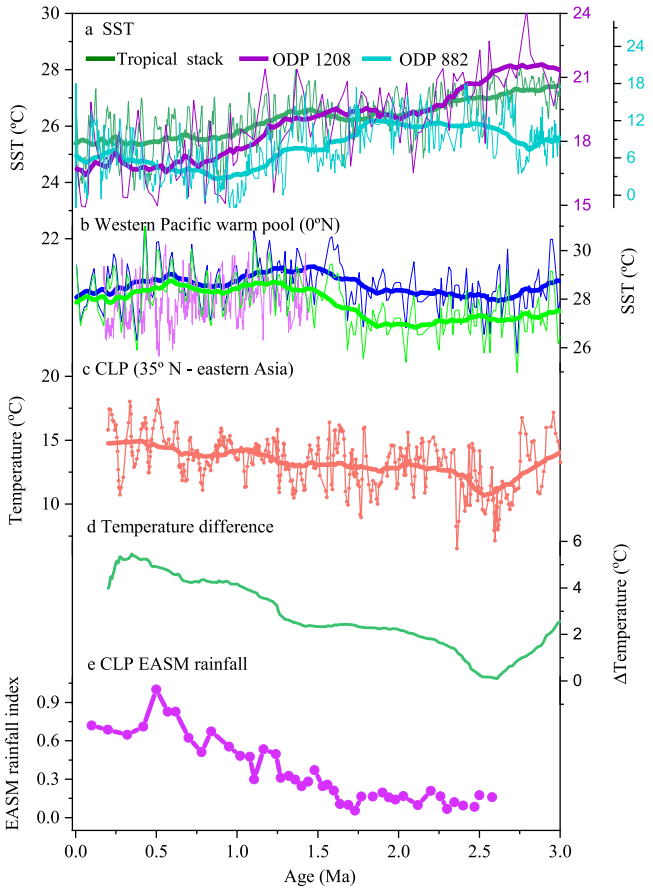

Figure 4. Correlation of land-sea thermal contrast with the long-term East Asian summer monsoon (EASM) over the past 3.0 Myr. (a) Ocean sea surface temperature (SST) records (Tropical SST stack, green, Herbert et al., 2010; alkenone-based SST records at ODP 1208, purple, LaRiviere et al., 2012, and ODP 882, blue, Martinez-Garcia et al., 2010, in the North Pacific). (b) Mg/Ca-SST records at ODP 806B (unadjusted, Wara et al., 2005, green; adjusted, Medina-Elizalde et al., 2008, blue; high-resolution, Medina-Elizalde & Lea, 2005, pink). (c) Land surface temperature (LST) on the Chinese Loess Plateau (CLP), three point-moving averaged. (d) Land-sea thermal difference. Temperature changes (ΔTemperature) are relative to values at 2.6 Ma. The land-sea thermal difference was calculated as the difference between the 400-Kyr running averages of LST record and of the Tropical SST stack record. (e) East Asian summer monsoon rainfall index from the Lingtai section (Meng et al., 2018). The heavy lines represent 400-Kyr running averages.

monsoonal and westerlies regions might be also linked to the increased zonal Pacific temperature gradient (W. Liu et al., 2020). Lastly, vegetation effect (Lu et al., 2019) exists particularly during deglacial/glacial periods in our CLP temperature record, and the long-term glacial EASM behavior remains to be debated. We thus leave the assessment of its relationship in glacial periods to future investigations, while the relationship of increased land-sea thermal contrast with the EASM enhancement for Pleistocene interglacial periods can be established here.

The gradual increasing land-sea thermal contrast documented in this study provides a simple and most parsimonious explanation for the long-term EASM enhancement over the Pleistocene interglacials (Text S1 and Figure S7 in Supporting Information S1). Without a warming continental temperature trend and an increasing land-sea temperature contrast, Meng et al. (2018) invoked the increase in the tropical Pacific zonal SST gradient (J. J. Liu et al., 2019; Tierney et al., 2019; Wara et al., 2005; Zhang et al., 2014) as a possible mechanism for the EASM increase during much of the Pleistocene. Zheng et al. (2022) also found that the early Pliocene drought conditions coincide with the occurrence of weakened zonal and meridional large-scale SST gradients in the Pacific Ocean. While this sea-based hypothesis is likely to explain the source of moisture in the equatorial ocean, a much stronger force is needed to deliver the moisture in penetrating the Asian inland by EASM under the global cooling climate trend indicated by SST data. Our new LST record reconciles the paradox by clearly showing that, under the long-term global cooling background, a steady warming LST would have increased the land-sea thermal contrast which serves as driving force for a stronger EASM during Pleistocene interglacial periods, while enhanced tropical SST gradient may have provided more moisture available in the western Pacific (Figure 4).

4. Conclusions

In summary, we reconstructed so far the longest continuous LST on Asian continent and found that a long-term warming trend during the early-middle Pleistocene is running to the opposite direction of the global ocean cooling trend. Our study shows that the unexpected land warming trend might represent a previously unrecognized long-term and large-scale climate phenomenon of increasing land-sea thermal contrast that provides a parsimonious explanation for the strengthening of EASM during much of the Pleistocene. In addition, although more continuous long-term terrestrial temperature records are urgently needed to better understand the mechanisms of the land warming phenomenon, a gradual land warming in monsoonal regions during the Pleistocene could have also played a consequential role in the dynamic of biological evolution and diversity, including the development of Pleistocene refugia and the diversification and migration of early human species.

Data Availability Statement

The data that support the findings of this study are made available through the East Asian Paleoenvironmental Science Database at http://paleodata.ieecas.cn/FrmDataInfo_EN.aspx?id=c5cbee6b-fe4c-4639-918b-8596de4a98a2 or through Figshare at https://figshare.com/articles/dataset/Lingtai_temperature/20411118.

Acknowledgments
The authors thank J. B. Dong, M. Xing, X. L. Ma, and J. J. Zhao for helpful discussions and X. K. Qiang and Y. H. H. He for their help in sampling. This research was supported by the Strategic Priority Research Program of Chinese Academy of Sciences (XDB40000000 and XDA2007020202), the CAS "Light of West China" (XAB2019A01), the National Natural Science Foundation of China (41991251), and Chinese Academy of Sciences (QYZDY-SSW-DQC001).

References

Abell, J. T., Winckler, G., Anderson, R. F., & Herbert, T. D. (2021). Poleward and weakened westerlies during Pliocene warmth. *Nature*, *589*(7840), 70–75. https://doi.org/10.1038/s41586-020-03062-1

Balsam, W., Ji, J. F., & Chen, J. (2004). Climatic interpretation of the Luochuan and Lingtai loess sections, China, based on changing iron oxide mineralogy and magnetic susceptibility. *Earth and Planetary Science Letters*, *223*(3–4), 335–348. https://doi.org/10.1016/j.epsl.2004.04.023

Chalk, T. B., Hain, M. P., Foster, G. L., Rohling, E. J., Sexton, P. F., Badger, M. P. S., et al. (2017). Causes of ice age intensification across the Mid-Pleistocene Transition. *Proceedings of the National Academy of Sciences of the United States of America*, *114*(50), 13114–13119. https://doi.org/10.1073/pnas.1702143114

Chiang, J. C. H., Fung, I. Y., Wu, C. H., Cai, Y. H., Edman, J. P., Liu, Y., et al. (2015). Role of seasonal transitions and westerly jets in East Asian paleoclimate. *Quaternary Science Reviews*, *108*, 111–129. https://doi.org/10.1016/j.quascirev.2014.11.009

Crampton-Flood, E. D., Tierney, J. E., Peterse, F., Kirkels, F. M. S. A., & Sinninghe Damsté, J. S. (2020). BayMBT. A Bayesian calibration model for branched glycerol dialkyl glycerol tetraethers in soils and peats. *Geochimica et Cosmochimica Acta*, *268*, 142–159. https://doi.org/10.1016/j.gca.2019.09.043

de Garidel-Thoron, T., Rosenthal, Y., Bassinot, F., & Beaufort, L. (2005). Stable sea surface temperatures in the western Pacific warm pool over the past 1.75 million years. *Nature*, *433*(7023), 294–298. https://doi.org/10.1038/nature03189

De Jonge, C., Hopmans, E. C., Zell, C. I., Kim, J. H., Schouten, S., & Sinninghe Damste, J. S. (2014). Occurrence and abundance of 6-methyl branched glycerol dialkyl glycerol tetraethers in soils. Implications for palaeoclimate reconstruction. *Geochimica et Cosmochimica Acta*, *141*, 97–112. https://doi.org/10.1016/j.gca.2014.06.013

Fang, X. M., An, Z. S., Clemens, S. C., Zan, J. B., Shi, Z. G., Yang, S., & Han, W. (2020). The 3.6-Ma aridity and westerlies history over midlatitude Asia linked with global climatic cooling. *Proceedings of the National Academy of Sciences of the United States of America*, *117*(40), 24729–24734. https://doi.org/10.1073/pnas.1922710117

Fedorov, A. V., Brierley, C. M., Lawrence, K. T., Liu, Z., Dekens, P. S., & Ravelo, A. C. (2013). Patterns and mechanisms of early Pliocene warmth. *Nature*, *496*(7443), 43–49. https://doi.org/10.1038/nature12003

Gao, L., Nie, J. S., Clemens, S., Liu, W. G., Sun, J. M., Zech, R., & Huang, Y. (2012). The importance of solar insolation on the temperature variations for the past 110 kyr on the Chinese Loess Plateau. *Palaeogeography, Palaeoclimatology, Palaeoecology*, *317*, 128–133. https://doi.org/10.1016/j.palaeo.2011.12.021

Haug, G. H., Ganopolski, A., Sigman, D. M., Rosell-Mele, A., Swann, G. E. A., Tiedemann, R., et al. (2005). North Pacific seasonality and the glaciation of North America 2.7 million years ago. *Nature*, *433*(7028), 821–825. https://doi.org/10.1038/nature03332

Herbert, T. D., Lawrence, K. T., Tzanova, A., Peterson, L. C., Caballero-Gill, R., & Kelly, C. S. (2016). Late Miocene global cooling and the rise of modern ecosystems. *Nature Geoscience*, *9*(11), 843–847. https://doi.org/10.1038/ngeo2813

Herbert, T. D., Peterson, L. C., Lawrence, K. T., & Liu, Z. H. (2010). Tropical ocean temperatures over the past 3.5 million years. *Science*, *328*(5985), 1530–1534. https://doi.org/10.1126/science.1185435

IPCC. (2019). *Climate change and land: An IPCC special report on climate change, desertification, land degradation, sustainable land management, food security, and greenhouse gas fluxes in terrestrial ecosystems*. In press.

Johnson, T. C., Werne, J., Brown, E. T., Abbott, A., Berke, M., Steinman, B. A., et al. (2016). A progressively wetter climate in southern East Africa over the past 1.3 million years. *Nature*, *537*(7619), 220–224. https://doi.org/10.1038/nature19065

Killick, R., & Eckley, I. A. (2015). changepoint. An R package for changepoint analysis. *Journal of Statistical Software*, *58*(3), 1–19. https://doi.org/10.18637/jss.v058.i03

LaRiviere, J., Ravelo, A. C., Crimmins, A., Dekens, S., Ford, H. L., Lyle, M., & Wara, M. W. (2012). Late Miocene decoupling of oceanic warmth and atmospheric carbon dioxide forcing. *Nature*, *486*(7401), 97–100. https://doi.org/10.1038/nature11200

Liang, J., Russell, J. M., Xie, H. C., Lupien, R. L., Si, G. C., Wang, J., et al. (2019). Vegetation effects on temperature calibrations of branched glycerol dialkyl glycerol tetraether (brGDGTs) in soils. *Organic Geochemistry*, *127*, 1–11. https://doi.org/10.1016/j.orggeochem.2018.10.010

Lisiecki, L. E., & Raymo, M. E. (2005). A Pliocene-Pleistocene stack of 57 globally distributed benthic $\delta^{18}O$ records. *Paleoceanography*, *20*(1), PA1003. https://doi.org/10.1029/2004pa001071

Liu, J. J., Tian, J., Liu, Z. H., Herbert, T. D., Fedorov, A. V., & Lyle, M. (2019). Eastern equatorial Pacific cold tongue evolution since the late Miocene linked to extratropical climate. *Science Advances*, *5*(4), eaau6060. https://doi.org/10.1126/sciadv.aau6060

Liu, T. S., & Ding, Z. L. (1998). Chinese loess and the paleomonsoon. *Annual Review of Earth and Planetary Sciences*, *26*(1), 111–145. https://doi.org/10.1146/annurev.earth.26.1.111

Liu, W., Liu, Z., Sun, J., Song, C., Chang, H., Wang, H., et al. (2020). Onset of permanent Taklimakan Desert linked to the mid-Pleistocene transition. *Geology*, *48*(8), 782–786. https://doi.org/10.1130/g47406.1

Lu, H. X., Liu, W. G., Yang, H., Wang, H. Y., Liu, Z. H., Leng, Q., et al. (2019). 800-kyr land temperature variations modulated by vegetation changes on Chinese Loess Plateau. *Nature Communications*, *10*(1), 1958. https://doi.org/10.1038/s41467-019-09978-1

Martinez-Garcia, A., Rosell-Mele, A., McClymont, E. L., Gersonde, R., & Haug, G. H. (2010). Subpolar link to the emergence of the modern equatorial Pacific cold tongue. *Science*, *328*(5985), 1550–1553. https://doi.org/10.1126/science.1184480

Medina-Elizalde, M., & Lea, D. W. (2005). The mid-Pleistocene transition in the tropical Pacific. *Science*, *310*(5750), 1009–1012. https://doi.org/10.1126/science.1115933

Medina-Elizalde, M., Lea, D. W., & Fantle, M. S. (2008). Implications of seawater Mg/Ca variability for Plio-Pleistocene tropical climate reconstruction. *Earth and Planetary Science Letters*, *269*(3–4), 584–594. https://doi.org/10.1016/j.epsl.2008.03.014

Meng, X. Q., Liu, L. W., Wang, X. T., Balsam, W., Chen, J., & Ji, J. (2018). Mineralogical evidence of reduced East Asian summer monsoon rainfall on the Chinese Loess Plateau during the early Pleistocene interglacials. *Earth and Planetary Science Letters*, *486*, 61–69. https://doi.org/10.1016/j.epsl.2017.12.048

Peterse, F., Martinez-Garcia, A., Zhou, B., Beets, C. J., Prins, M. A., Zheng, H., & Eglinton, T. I. (2014). Molecular records of continental air temperature and monsoon precipitation variability in East Asia spanning the past 130,000 years. *Quaternary Science Reviews*, *83*, 76–82. https://doi.org/10.1016/j.quascirev.2013.11.001

Peterse, F., Prins, M. A., Beets, C. J., Troelstra, S. R., Zheng, H. B., Gu, Z., et al. (2011). Decoupled warming and monsoon precipitation in East Asia over the last deglaciation. *Earth and Planetary Science Letters*, *301*(1–2), 256–264. https://doi.org/10.1016/j.epsl.2010.11.010

Ruddiman, W. F., Raymo, M. E., Martinson, D. G., Clement, B. M., & Backman, J. (1989). Pleistocene evolution: Northern hemisphere ice sheets and North Atlantic Ocean. *Paleoceanography*, *4*(4), 353–412. https://doi.org/10.1029/pa004i004p00353

Snyder, C. W. (2016). Evolution of global temperature over the past two million years. *Nature*, *538*(7624), 226–228. https://doi.org/10.1038/nature19798

Sun, Y. B., & An, Z. S. (2005). Late Pliocene-Pleistocene changes in mass accumulation rates of eolian deposits on the central Chinese Loess Plateau. *Journal of Geophysical Research*, *110*(D23), D23101. https://doi.org/10.1029/2005jd006064

Sun, Y. B., Clemens, S. C., An, Z. S., & Yu, Z. W. (2006). Astronomical timescale and palaeoclimatic implication of stacked 3.6-Myr monsoon records from the Chinese Loess Plateau. *Quaternary Science Reviews*, *25*(1–2), 33–48. https://doi.org/10.1016/j.quascirev.2005.07.005

Tang, C. Y., Yang, H., Pancost, R. D., Griffiths, M. L., Xiao, G. Q., Dang, X., & Xie, S. (2017). Tropical and high latitude forcing of enhanced megadroughts in Northern China during the last four terminations. *Earth and Planetary Science Letters*, *479*, 98–107. https://doi.org/10.1016/j.epsl.2017.09.012

Thomas, E. K., Clemens, S. C., Sun, Y. B., Huang, Y. S., Prell, W., Chen, G., et al. (2017). Midlatitude land surface temperature impacts the timing and structure of glacial maxima. *Geophysical Research Letters*, *44*(2), 984–992. https://doi.org/10.1002/2016gl071882

Tian, J., Xie, X., Ma, W. T., Jin, H. Y., & Wang, X. (2011). X-ray fluorescence core scanning records of chemical weathering and monsoon evolution over the past 5 Myr in the southern South China Sea. *Paleoceanography*, *26*(4), PA4202. https://doi.org/10.1029/2010pa002045

Tierney, J. E., Haywood, A. M., Feng, R., Bhattacharya, T., & Otto-Bliesner, B. L. (2019). Pliocene warmth consistent with greenhouse gas forcing. *Geophysical Research Letters*, *46*(15), 9136–9144. https://doi.org/10.1029/2019gl083802

Véquaud, P., Thibault, A., Derenne, S., Anquetil, C., Collin, S., Contreras, S., et al. (2022). FROG. A global machine-learning temperature calibration for branched GDGTs in soils and peats. *Geochimica et Cosmochimica Acta*, *318*, 468–494. https://doi.org/10.1016/j.gca.2021.12.007

Wang, H. Y., An, Z. S., Lu, H. X., Zhao, Z. H., & Liu, W. G. (2020). Calibrating bacterial tetraether distributions towards in situ soil temperature and application to a loess-paleosol sequence. *Quaternary Science Reviews*, *231*, 106172. https://doi.org/10.1016/j.quascirev.2020.106172

Wara, M. W., Ravelo, A. C., & Delaney, M. L. (2005). Permanent El Nino-like conditions during the Pliocene warm period. *Science*, *309*(5735), 758–761. https://doi.org/10.1126/science.1112596

Zhang, Y. G., Pagani, M., & Liu, Z. H. (2014). A 12-million-year temperature history of the tropical Pacific ocean. *Science*, *344*(6179), 84–87. https://doi.org/10.1126/science.1246172

Zhao, Y., Liang, C., Cui, Q. Y., Qin, F., Zheng, Z., Xiao, X., et al. (2021). Temperature reconstructions for the last 1.74-Ma on the eastern Tibetan Plateau based on a novel pollen-based quantitative method. *Global and Planetary Change*, *199*(8), 103433. https://doi.org/10.1016/j.gloplacha.2021.103433

Zheng, Y., Fedorov, A. V., Burls, N. J., Zhang, R., Brierley, C. M., Fang, Z., et al. (2022). Severe drought conditions in northern East Asia during the early Pliocene caused by weakened Pacific meridional temperature gradient. *Geophysical Research Letters*, *49*(14), e2022GL098813. https://doi.org/10.1029/2022gl098813

References From the Supporting Information

An, Z., Kukla, G. J., Porter, S. C., & Xiao, J. (1991). Magnetic susceptibility evidence of monsoon variation on the Loess Plateau of central China during the last 130,000 years. *Quaternary Research*, *36*(1), 29–36. https://doi.org/10.1016/0033-5894(91)90015-W

Ao, H., Dekkers, M. J., Qin, L., & Xiao, G. Q. (2011). An updated astronomical timescale for the Plio-Pleistocene deposits from South China Sea and new insights into Asian monsoon evolution. *Quaternary Science Reviews*, *30*(13–14), 1560–1575. https://doi.org/10.1016/j.quascirev.2011.04.009

Broecker, W. S., & Putnam, A. E. (2013). Hydrologic impacts of past shifts of Earth's thermal equator offer insight into those to be produced by fossil fuel CO_2. *Proceedings of the National Academy of Sciences*, *110*(42), 16710–16715. https://doi.org/10.1073/pnas.1301855110

Chang, C., Zhang, Y. S., & Li, T. (2000). Interannual and interdecadal variations of the East Asian summer monsoon and tropical Pacific SSTs. Part II. Meridional structure of the monsoon. *Journal of Climate*, *13*(24), 4326–4340. https://doi.org/10.1175/1520-0442(2000)013<4326:iaivot>2.0.co;2

Chen, J., Wang, Y. J., Chen, Y., Liu, L. W., Ji, J. F., & Huayu, L. (2000). Rb and Sr geochemical characterization of the Chinese Loess stratigraphy and its implications for palaeomonsoon climate. *Acta Geologica Sinica-English Edition*, *74*(2), 279–288. https://doi.org/10.1111/j.1755-6724.2000.tb00462.x

Cheng, H., Edwards, R. L., Sinha, A., Spotl, C., Yi, L., Chen, S., et al. (2016). The Asian monsoon over the past 640,000 years and ice age terminations. *Nature*, *534*(7609), 640–646. https://doi.org/10.1038/nature18591

Clift, D., Hodges, K., Heslop, D., Hannigan, R., Van Long, H., & Calves, G. (2008). Correlation of Himalayan exhumation rates and Asian monsoon intensity. *Nature Geoscience*, *1*(12), 875–880. https://doi.org/10.1038/ngeo351

Dang, X. Y., Yang, H., Naafs, B. D. A., Pancost, R. D., & Xie, S. C. (2016). Evidence of moisture control on the methylation of branched glycerol dialkyl glycerol tetraethers in semi-arid and arid soils. *Geochimica et Cosmochimica Acta*, *189*, 24–36. https://doi.org/10.1016/j.gca.2016.06.004

Davtian, N., Menot, G., Bard, E., Poulenard, J., & Podwojewski, P. (2016). Consideration of soil types for the calibration of molecular proxies for soil pH and temperature using global soil datasets and Vietnamese soil profiles. *Organic Geochemistry*, *101*, 140–153. https://doi.org/10.1016/j.orggeochem.2016.09.002

Duan, Y., Sun, Q., Werne, J. P., Hou, J., Yang, H., Wang, Q., et al. (2022). The impact of precipitation on the distributions of branched tetraethers in alkaline soils. *Organic Geochemistry*, *169*, 104410. https://doi.org/10.1016/j.orggeochem.2022.104410

Duan, Y. W., Sun, Q., Werne, J. P., Zhao, H., Zhang, D. J., Zhang, N., et al. (2019). Mid-Holocene moisture maximum revealed by pH changes derived from branched tetraethers in loess deposits of the northeastern Tibetan Plateau. *Palaeogeography, Palaeoclimatology, Palaeoecology*, *520*, 138–149. https://doi.org/10.1016/j.palaeo.2019.01.034

Farnsworth, A., Lunt, D., Robinson, S. A., Valdes, P. J., Roberts, W. H., Clift, P. D., et al. (2019). Past East Asian monsoon evolution controlled by paleogeography, not CO_2. *Science Advances*, *5*(10), eaax1697. https://doi.org/10.1126/sciadv.aax1697

Huguet, A., Fosse, C., Metzger, P., Fritsch, E., & Derenne, S. (2010). Occurrence and distribution of non-extractable glycerol dialkyl glycerol tetraethers in temperate and tropical podzol profiles. *Organic Geochemistry*, *41*(8), 833–844. https://doi.org/10.1016/j.orggeochem.2010.04.020

Kukla, G., & An, Z. S. (1989). Loess stratigraphy in central China. *Palaeogeography, Palaeoclimatology, Palaeoecology*, *72*(1–2), 203–225. https://doi.org/10.1016/0031-0182(89)90143-0

Logan, G. A., Smiley, C. J., & Eglinton, G. (1995). Preservation of fossil leaf waxes in association with their source tissues, Clarkia, Northern Idaho, USA. *Geochimica et Cosmochimica Acta*, *59*(4), 751–763. https://doi.org/10.1016/0016-7037(94)00362-p

Lorenz, S. J., Kim, J. H., Rimbu, N., Schneider, R. R., & Lohmann, G. (2006). Orbitally driven insolation forcing on Holocene climate trends: Evidence from alkenone data and climate modeling. *Paleoceanography*, *21*(1), PA1002. https://doi.org/10.1029/2005pa001152

Lu, H. X., Liu, W. G., Wang, H. Y., & Wang, Z. (2016). Variation in 6-methyl branched glycerol dialkyl glycerol tetraethers in Lantian loess-paleosol sequence and effect on paleotemperature reconstruction. *Organic Geochemistry*, *100*, 10–17. https://doi.org/10.1016/j.orggeochem.2016.07.006

Lü, X. X., Liu, X. L., Elling, F. J., Yang, H., Xie, S. C., Song, J., et al. (2015). Hydroxylated isoprenoid GDGTs in Chinese coastal seas and their potential as a paleotemperature proxy for mid-to-low latitude marginal seas. *Organic Geochemistry*, *89–90*, 31–43. https://doi.org/10.1016/j.orggeochem.2015.10.004

Peaple, M. D., Beverly, E. J., Garza, B., Baker, S., Levin, N. E., Tierney, J. E., et al. (2022). Identifying the drivers of GDGT distributions in alkaline soil profiles within the Serengeti ecosystem. *Organic Geochemistry*, *169*, 104433. https://doi.org/10.1016/j.orggeochem.2022.104433

Sessions, A. L., Burgoyne, T. W., Schimmelmann, A., & Hayes, J. M. (1999). Fractionation of hydrogen isotopes in lipid biosynthesis. *Organic Geochemistry*, *30*(9), 1193–1200. https://doi.org/10.1016/s0146-6380(99)00094-7

Sun, D. G., An, Z. S., Shaw, J., Bloemendal, J., & Sun, Y. B. (1998). Magnetostratigraphy and palaeoclimatic significance of late tertiary aeolian sequences in the Chinese Loess Plateau. *Geophysical Journal International*, *134*(1), 207–212. https://doi.org/10.1046/j.1365-246x.1998.00553.x

Thomson, J. R., Holden, B., Anand, P., Edwards, N. R., Porchier, C. A., & Harris, N. B. W. (2021). Tectonic and climatic drivers of Asian monsoon evolution. *Nature Communications*, *12*(1), 4022. https://doi.org/10.1038/s41467-021-24244-z

Wang, B., Wu, R. G., & Fu, X. H. (2000). Pacific-East Asian teleconnection: How does ENSO affect East Asian climate? *Journal of Climate*, *13*(9), 1517–1536. https://doi.org/10.1175/1520-0442(2000)013<1517:peathd>2.0.co;2

Wang, H. Y., Liu, W. G., & Lu, H. X. (2016). Appraisal of branched glycerol dialkyl glycerol tetraether-based indices for North China. *Organic Geochemistry*, *98*, 118–130. https://doi.org/10.1016/j.orggeochem.2016.05.013

Wang, Y. J., Cheng, H., Edwards, R. L., Kong, X. G., Shao, X. H., Chen, S., et al. (2008). Millennial- and orbital-scale changes in the East Asian monsoon over the past 224,000 years. *Nature*, *451*(7182), 1090–1093. https://doi.org/10.1038/nature06692

Wang, Z., Liu, W. G., Wang, H., Cao, Y. N., Hu, J., Dong, J., et al. (2021). New chronology of the Chinese loess-paleosol sequence by leaf wax δD records during the past 800 k.y. *Geology*, *49*(7), 847–850. https://doi.org/10.1130/g48833.1

Wu, F. L., Fang, X. M., Ma, Y. Z., Herrmann, M., Mosbrugger, V., An, Z., & Miao, Y. (2007). Plio-Quaternary stepwise drying of Asia. Evidence from a 3-Ma pollen record from the Chinese Loess Plateau. *Earth and Planetary Science Letters*, *257*(1–2), 160–169. https://doi.org/10.1016/j.epsl.2007.02.029

Yamamoto, Y., Ajioka, T., & Yamamoto, M. (2016). Climate reconstruction based on GDGT-based proxies in a paleosol sequence in Japan: Post-depositional effect on the estimation of air temperature. *Quaternary International*, *397*, 380–391. https://doi.org/10.1016/j.quaint.2014.12.009

Yang, H., Pancost, R. D., Dang, X. Y., Zhou, X. Y., Evershed, R., Xiao, G., et al. (2014). Correlations between microbial tetraether lipids and environmental variables in Chinese soils: Optimizing the paleo-reconstructions in semi-arid and arid regions. *Geochimica et Cosmochimica Acta*, *126*, 49–69. https://doi.org/10.1016/j.gca.2013.10.041

Zech, R., Gao, L., Tarozo, R., & Huang, Y. (2012). Branched glycerol dialkyl glycerol tetraethers in Pleistocene loess-paleosol sequences: Three case studies. *Organic Geochemistry*, *53*, 38–44. https://doi.org/10.1016/j.orggeochem.2012.09.005

Zhang, J., Li, J. J., Guo, B. H., Ma, Z. H., Li, X. M., Ye, X., et al. (2016). Magnetostratigraphic age and monsoonal evolution recorded by the thickest Quaternary loess deposit of the Lanzhou region, western Chinese Loess Plateau. *Quaternary Science Reviews*, *139*, 17–29. https://doi.org/10.1016/j.quascirev.2016.02.025